
MTS-Mixers: Multivariate Time Series Forecasting via Factorized Temporal and Channel Mixing

Zhe Li¹ Zhongwen Rao² Lujia Pan² Zenglin Xu¹

Abstract

Multivariate time series forecasting has been widely used in various practical scenarios. Recently, Transformer-based models have shown significant potential in forecasting tasks due to the capture of long-range dependencies. However, recent studies in the vision and NLP fields show that the role of attention modules is not clear, which can be replaced by other token aggregation operations. This paper investigates the contributions and deficiencies of attention mechanisms on the performance of time series forecasting. Specifically, we find that (1) attention is not necessary for capturing temporal dependencies, (2) the entanglement and redundancy in the capture of temporal and channel interaction affect the forecasting performance, and (3) it is important to model the mapping between the input and the prediction sequence. To this end, we propose MTS-Mixers, which use two factorized modules to capture temporal and channel dependencies. Experimental results on several real-world datasets show that MTS-Mixers outperform existing Transformer-based models with higher efficiency.

1. Introduction

Multivariate time series forecasting has been an increasingly popular topic in various scenarios, such as electricity forecasting (Khan et al., 2020), weather forecasting (Angryk et al., 2020), and traffic flow estimation (Chen et al., 2001). With the scaling of computing resources and model architectures, deep learning techniques, including RNN-based (Lai et al., 2018) and CNN-based models (Bai et al., 2018), have achieved better prediction performance than traditional statistical methods (Zhang, 2003; Ariyo et al.,

2014). Due to the capture of long-range dependencies, Transformer (Vaswani et al., 2017) has been recently used to catch long-term temporal correlation in time series forecasting and has demonstrated promising results (Zhou et al., 2021; Wu et al., 2021; Liu et al., 2022b; Zhou et al., 2022). The overall architecture of existing Transformer-based models on time series forecasting is illustrated in Figure 1. In the embedding module, the input time series are generally fed into one 1D convolutional layer to generate temporal tokens with positional or date-specific encoding at the point level for preserving ordering information. Then the encoder will capture the temporal interaction among time points via an attention-like mechanism, and the decoder will generate the prediction sequence in one pass.

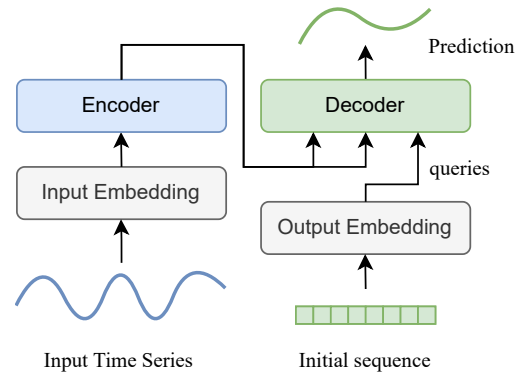


Figure 1. The overall architecture of Transformer-based models for time series forecasting. Notice that the generation of the prediction sequence in the decoder is non-autoregressive.

Although these Transformer-based models perform well on long-term time series forecasting tasks, there are still some problems to be addressed. First, there is a lack of explanation about the attention mechanism for capturing temporal dependency. A simple yet effective baseline DLinear (Zeng et al., 2022) questioned whether Transformer-based models are effective for time series forecasting. Second, Transformer-based models heavily rely on additional positional or date-specific encoding to guarantee the ordering of attention score, which may disturb the capture of temporal interaction. Third, while existing Transformer-based methods almost concentrate on how to reduce the

¹Harbin Institute of Technology, Shenzhen ²Huawei Technologies Ltd.. Correspondence to: Zhe Li <plum271828@gmail.com>, Zhongwen Rao <raozhongwen@huawei.com>, Lujia Pan <panlujia@huawei.com>, Zenglin Xu <zenglin@gmail.com>.

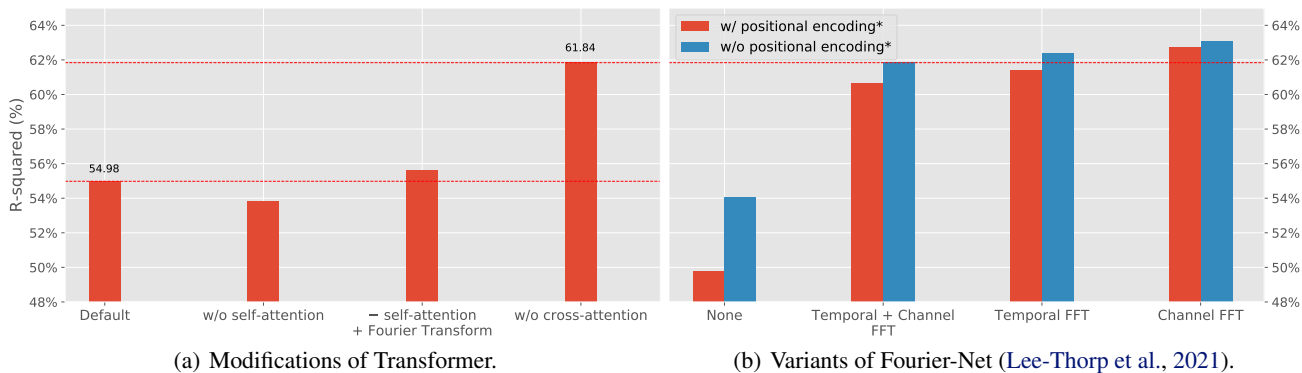
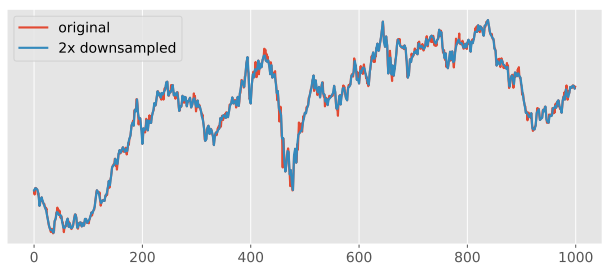


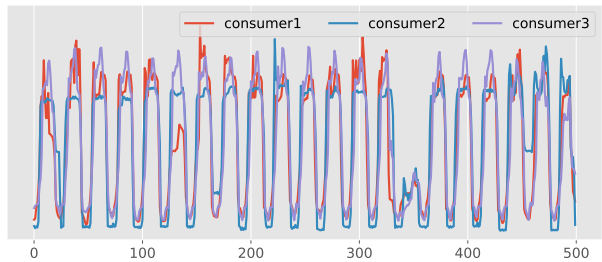
Figure 2. ETTh1 (Zhou et al., 2021) forecasting results of the modifications on Transformer and variants of Fourier-Net at 96-96 setting (The length of the historical horizon is set as 96 and the prediction length is 96). The higher R-squared score indicates better performance.

complexity of attention computation, and have designed various sparse attention mechanisms through proper selection strategies to attain $O(L \log L)$ even $O(L)$ time and memory complexity where L denotes the length of input sequence. However, these methods have a bulk of additional operations beyond attention, which makes the actual running time very long. To verify the effectiveness of the attention mechanism on time series forecasting, we conduct a group of experiments on ETTh1 (Zhou et al., 2021). Figure 2(a) provides the forecasting results of the modifications on the Transformer. We can see that directly replacing the attention layer with Fourier Transform maintains the forecasting performance and removing the cross-attention significantly improves it. These results indicate that the attention mechanism on time series forecasting tasks may not be that effective. Figure 2(b) shows that applying a simple Fourier Transform can achieve the same, even better forecasting performance compared with attention-based models without extra positional or date-specific encoding. Additionally, individually capturing temporal and channel dependencies may bring extra improvement.

Moreover, due to the difference in the sampling rate and the number of sensors, the current multivariate time series data from different scenarios often vary greatly in data form and have serious redundancy. Consider one instance of collected time series data as a tensor $\mathcal{X} \in \mathbb{R}^{n \times c}$, where n denotes the length of \mathcal{X} and c is the dimension size. It is often uncertain which one is bigger or smaller between n and c . That is, \mathcal{X} generally has the low-rank property, such that $\text{rank}(\mathcal{X}) \ll \min(n, c)$. Figure 3 illustrates the ubiquitous redundancy of temporal and channel information. Specifically, the redundancy in temporal information is reflected in that the original sequence and the down-sampled sequence almost maintain the same temporal characteristics. The redundancy across channels occurs in that the information described by each channel may be consistent. Motivated



(a) The redundancy of temporal information.



(b) The redundancy across different channels.

Figure 3. The redundancy of existing multivariate time series data. **top**: Exchange rate under different sampling rates. **bottom**: Electricity consumption of three consumers.

by the above observations, we propose a novel and general framework for multivariate time series forecasting, named MTS-Mixers. The main contributions of this paper are:

- We investigate the attention mechanism in time series forecasting and propose a novel and general framework named MTS-Mixers, which respectively capture temporal and channel dependencies.
- We leverage the low-rank property of existing time series data via factorized temporal and channel mixing and attain better prediction accuracy and efficiency.

- MTS-Mixers has achieved state-of-the-art forecasting performance on several public real-world multivariate time series datasets, yielding a 15.4% MSE and a 12.9% MAE reduction on average.

2. Related Work

Due to the ability of the attention mechanism to capture long-range dependencies, Transformer-based models have been widely used in language and vision tasks. Song et al. (2018); Ma et al. (2019); Li et al. (2019) tried to directly apply vanilla Transformer to time series data but failed in long sequence forecasting tasks as self-attention operation scales quadratically with the input sequence length. Child et al. (2019) applied sparse attention to reducing time complexity and memory usage for processing longer sequences. Zhou et al. (2021) introduced non-autoregressive decoding to generate future time series to be predicted in one pass and designed selective attention for higher efficiency. Liu et al. (2022b) proposed tree structure pyramidal attention for lower complexity. To enhance the capture of temporal dependency, Wu et al. (2021); Woo et al. (2022); Zhou et al. (2022) disentangled time series data into trend and seasonality parts by removing the moving average and introduced frequency domain transformation. Recently, a simple but effective baseline (Zeng et al., 2022) questioned whether Transformers are effective for time series forecasting, reminding us to rethink the role of the attention mechanism.

Apart from the dot product attention mechanism, it is shown in Synthesizer (Tay et al., 2020), MLP-Mixer (Tolstikhin et al., 2021), FNet (Lee-Thorp et al., 2021) and Poolformer (Diao et al., 2022) that, by replacing attention in Transformer with spatial MLP, Fourier Transform and pooling layer, the resulting models will deliver competitive performance in machine translation and computer vision domain. Unlike mentioned works above, we first investigate what we actually learn from attention-like modules in time series forecasting tasks, and then propose MTS-Mixers with factorized temporal and channel mixing to fit the inherent low-rank property of time series data.

3. Preliminary

3.1. Problem definition

Given a historical multivariate time series instance $\mathcal{X}_h = [\mathbf{x}_1, \mathbf{x}_2, \dots, \mathbf{x}_n] \in \mathbb{R}^{n \times c}$ with the length of n , time series forecasting tasks aim to predict the next m steps values $\mathcal{X}_f = [\mathbf{x}_{n+1}, \mathbf{x}_{n+2}, \dots, \mathbf{x}_{n+m}] \in \mathbb{R}^{m \times c}$ across all the c channels. Forecasting tasks are required to learn a map $\mathcal{F} : \mathcal{X}_h^{n \times c} \mapsto \mathcal{X}_f^{m \times c}$ where \mathcal{X}_h and \mathcal{X}_f are consecutive.

3.2. Rethinking the mechanism of attention in Transformer-based forecasting models

The general workflow of existing Transformer-based methods on time series forecasting tasks is illustrated in Figure 1. First, we generally utilize a 1D convolutional layer to obtain the input embedding $\mathcal{X}_{in} \in \mathbb{R}^{n \times d}$ from the original time series $\mathcal{X}_h \in \mathbb{R}^{n \times c}$ with the positional or date-specific encoding. Then on the encoder side, self-attention or other correlation patterns are used to capture token-level temporal similarity as

$$\tilde{\mathcal{X}} = \text{softmax}\left(\frac{\mathcal{X}_{in} \cdot \mathcal{X}_{in}^\top}{\sqrt{d}}\right) \cdot \mathcal{X} = R_1 \cdot \mathcal{X}_{in}, \quad (1)$$

where $R_1 \in \mathbb{R}^{n \times n}$ describes token-wise temporal information. A feedforward neural network with two linear layers and activation function will be applied on $\tilde{\mathcal{X}}$ to learn channel-wise features. On the decoder side, an initialized query $Q \in \mathbb{R}^{m \times d}$ is used to generate forecasting results as

$$\tilde{\mathcal{X}}_f = \text{softmax}\left(\frac{Q \cdot \tilde{\mathcal{X}}^\top}{\sqrt{d}}\right) \cdot \tilde{\mathcal{X}} = R_2 \cdot \tilde{\mathcal{X}}, \quad (2)$$

where $R_2 \in \mathbb{R}^{m \times n}$ describes the relationship between the input historical time series and the output prediction series. A projection layer is applied on $\tilde{\mathcal{X}}_f$ to obtain the final forecasting target $\mathcal{X}_f \in \mathbb{R}^{m \times c}$.

In essence, Transformer-based methods for time series forecasting contain two stages: learning token-wise temporal dependency across channels, and learning a map between input time series and output forecasting results. However, as shown in Figure 2, removing self-attention or cross-attention can maintain or even improve the forecasting performance. Replacing self-attention with Fourier Transform also delivers similar results, and respectively modeling temporal and channel dependencies will further enhance it. This means what we learn from attention-like modules is temporal dependency across all channels, and cross-attention bridges the relationship between input and output sequences. Attention mechanisms may not be necessary for capturing temporal dependency. Learning the mapping between input and output sequences and disentangling the modeling of temporal and channel dependencies may lead to better forecasting performance.

4. MTS-Mixers

This section introduces MTS-Mixers, our proposed general framework for time series forecasting that respectively captures temporal and channel dependencies. The overall architecture of MTS-Mixers is shown in Figure 4, which aims to learn a map between the input $\mathcal{X}_h \in \mathbb{R}^{n \times c}$ and the output $\mathcal{X}_f \in \mathbb{R}^{m \times c}$. Notably, the input embedding module is optional. For better understanding, filters such as convolutional layers and the attention are simplified as a module for

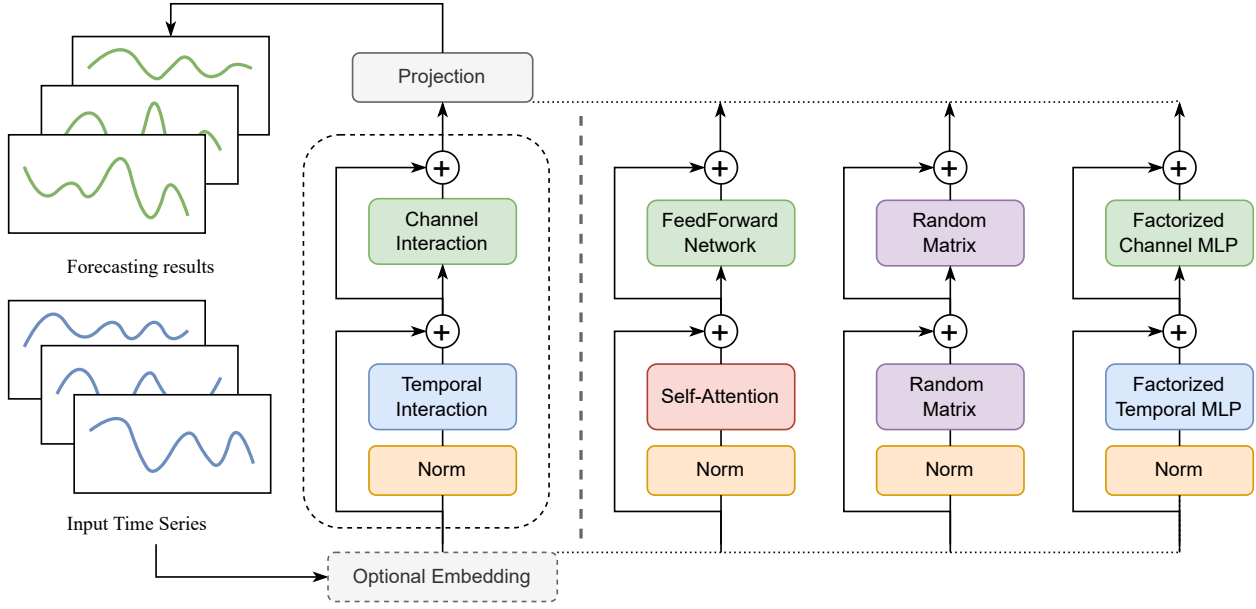


Figure 4. The overall architecture of MTS-Mixers. **Left:** the modules in the dashed box describe the general framework. **Right:** three specific implementations, where we can use attention, random matrix, or factorized MLP to capture dependencies.

capturing temporal interaction. Then the other module for catching channel interaction is also applied, and the linear projection layer outputs the final forecasting results. Equation (3) depicts the above simplified time series forecasting process.

$$\begin{aligned}\mathcal{X}_h^T &= \text{Temporal}(\text{norm}(\mathcal{X}_h)), \\ \mathcal{X}_h^C &= \text{Channel}(\mathcal{X}_h + \mathcal{X}_h^T), \\ \mathcal{X}_f &= \text{Linear}(\mathcal{X}_h^T + \mathcal{X}_h^C).\end{aligned}\quad (3)$$

In this paper, we provide three specific implementations of MTS-Mixers. More details of them are as follows.

Attention-based MTS-Mixer. As Equation (4) shows, we add the sinusoidal positional encoding to obtain the input embedding $\tilde{\mathcal{X}}_h$. Then, the multi-head self-attention will be used to capture temporal dependency \mathcal{X}_h^T . A feed-forward network is to learn the channel interaction \mathcal{X}_h^C . Compared with the vanilla Transformer, we remove its decoder and use one linear layer to directly learn the map between the learned features and the prediction sequence.

$$\begin{aligned}\tilde{\mathcal{X}}_h &= \text{norm}(\mathcal{X}_h) + \text{PE}(\mathcal{X}_h), \\ \mathcal{X}_h^T &= \text{Attention}(\tilde{\mathcal{X}}_h, \tilde{\mathcal{X}}_h, \tilde{\mathcal{X}}_h), \\ \mathcal{X}_h^C &= \text{FFN}(\tilde{\mathcal{X}}_h + \mathcal{X}_h^T).\end{aligned}\quad (4)$$

Random matrix MTS-Mixer. As mentioned in Section 3.2, what we need to learn from the input \mathcal{X}_h is three matrices: $T \in \mathbb{R}^{n \times n}$ describes the temporal dependency,

$C \in \mathbb{R}^{c \times c}$ describes the channel dependency and the projection $F \in \mathbb{R}^{m \times n}$ with the optional bias or activation. Equation (5) demonstrates a time series forecasting process via matrix multiplication as

$$\mathcal{X}_f = F \cdot \sigma(T) \cdot \mathcal{X}_h \cdot \phi(C), \quad (5)$$

where the operators σ and ϕ denote the optional added bias or activation. Because the initialization of the matrices F , T , and C are controllable, we call it a random matrix MTS-Mixer. The experiments in Section 5.3 analyze the impact of different methods of initialization.

Factorized temporal and channel mixing. Given the low-rank property of time series data described in Section 1, we design the factorized temporal and channel mixing strategies to capture dependencies with less redundancy. Specifically for the time series data with the temporal redundancy, we extract the temporal dependencies as Equation (6)

$$\begin{aligned}\mathcal{X}_{h,1}, \dots, \mathcal{X}_{h,s} &= \text{sampled}(\text{norm}(\mathcal{X}_h)), \\ \mathcal{X}_{h,i}^T &= \text{Temporal}(\mathcal{X}_{h,i}) \quad i \in [1, s], \\ \mathcal{X}_h^T &= \text{merge}(\mathcal{X}_{h,1}^T, \dots, \mathcal{X}_{h,s}^T),\end{aligned}\quad (6)$$

where we first equidistantly downsample the original time series into s interleaved subsequences. Then we individually utilize one temporal feature extractor (e.g., MLP or attention) to learn temporal information of those subsequences and merge them in the original order. For the time series data with channel redundancy, we reduce the noise of tensors corresponding to the time series in channel dimension

Table 1. Multivariate time series forecasting results. The length of the historical horizon is set as 36 for ILI and 96 for the others. The prediction lengths are {24,36,48,60} for ILI and {96, 192, 336, 720} for others. The best results are highlighted in **bold**.

Method	MTS-Mixers		FEDformer		DLinear		SCINet		Pyraformer		Autoformer		Informer		
Metric	MSE	MAE	MSE	MAE	MSE	MAE	MSE	MAE	MSE	MAE	MSE	MAE	MSE	MAE	
ECL	96	0.146	0.246	0.193	0.308	0.199	<u>0.284</u>	0.205	0.312	0.386	0.449	0.201	0.317	0.274	0.368
	192	0.163	0.260	0.201	0.315	0.198	<u>0.287</u>	<u>0.197</u>	0.308	0.378	0.443	0.222	0.334	0.296	0.386
	336	0.175	0.273	0.214	0.329	0.210	<u>0.302</u>	<u>0.202</u>	0.312	0.376	0.443	0.231	0.338	0.300	0.394
	720	0.202	0.295	0.246	0.355	0.245	<u>0.335</u>	<u>0.234</u>	0.338	0.376	0.445	0.254	0.361	0.373	0.439
	Avg.	0.172	0.269	0.214	0.327	0.213	<u>0.302</u>	<u>0.210</u>	0.318	0.379	0.445	0.227	0.338	0.311	0.397
Traffic	96	0.516	0.339	<u>0.587</u>	<u>0.366</u>	0.650	0.396	0.651	0.393	0.867	0.468	0.613	0.388	0.719	0.391
	192	0.521	0.353	<u>0.604</u>	<u>0.373</u>	0.605	0.378	0.604	0.372	0.869	0.467	0.616	0.382	0.696	0.379
	336	0.557	0.358	0.621	0.383	<u>0.612</u>	<u>0.382</u>	0.611	0.375	0.881	0.469	0.622	0.387	0.777	0.420
	720	0.578	0.369	<u>0.626</u>	<u>0.382</u>	<u>0.645</u>	<u>0.394</u>	0.649	0.393	0.896	0.473	0.660	0.408	0.864	0.472
	Avg.	0.543	0.355	<u>0.609</u>	<u>0.376</u>	0.628	0.388	0.629	0.383	0.878	0.469	0.628	0.391	0.764	0.415
PeMS04	96	0.349	0.309	<u>0.427</u>	<u>0.382</u>	0.725	0.560	0.554	0.410	0.621	0.469	1.183	0.772	0.578	0.440
	192	0.378	0.333	<u>0.449</u>	<u>0.396</u>	0.749	0.577	0.629	0.446	0.658	0.491	1.217	0.799	0.631	0.466
	336	0.387	0.343	<u>0.464</u>	<u>0.402</u>	0.680	0.528	0.611	0.442	0.626	0.463	1.587	0.934	0.666	0.489
	720	0.431	0.363	<u>0.521</u>	<u>0.446</u>	0.750	0.568	0.713	0.496	0.711	0.510	1.696	0.969	0.752	0.536
	Avg.	0.386	0.337	<u>0.465</u>	<u>0.407</u>	0.726	0.558	0.627	0.449	0.654	0.483	1.421	0.869	0.657	0.483
Exchange	96	0.079	0.197	0.148	0.278	<u>0.088</u>	<u>0.218</u>	0.142	0.249	1.748	1.105	0.197	0.323	0.847	0.752
	192	0.172	0.295	0.271	0.380	<u>0.176</u>	<u>0.315</u>	0.261	0.364	1.874	1.151	0.300	0.369	1.204	0.895
	336	<u>0.321</u>	0.409	0.460	0.500	0.313	<u>0.427</u>	0.457	0.490	1.943	1.172	0.509	0.524	1.672	1.036
	720	<u>0.842</u>	0.690	1.195	0.841	0.839	<u>0.695</u>	1.364	0.859	2.085	1.206	1.447	0.941	2.478	1.310
	Avg.	0.354	0.398	0.519	0.500	0.354	<u>0.414</u>	0.556	0.491	1.913	1.159	0.613	0.539	1.550	0.998
Weather	96	0.162	0.207	0.217	0.296	<u>0.196</u>	<u>0.255</u>	0.239	0.271	0.622	0.556	0.266	0.336	0.300	0.384
	192	0.208	0.250	0.276	0.336	<u>0.237</u>	<u>0.296</u>	0.283	0.303	0.739	0.624	0.307	0.367	0.598	0.544
	336	0.268	0.294	0.339	0.380	<u>0.283</u>	<u>0.335</u>	0.330	0.335	1.004	0.753	0.359	0.395	0.578	0.523
	720	0.346	0.345	0.403	0.428	<u>0.347</u>	<u>0.383</u>	0.400	0.379	1.420	0.934	0.419	0.428	1.059	0.741
	Avg.	0.246	0.274	0.309	0.360	<u>0.266</u>	<u>0.317</u>	0.313	0.322	0.946	0.717	0.338	0.382	0.634	0.548
ILI	24	1.677	0.799	3.228	1.260	<u>2.398</u>	<u>1.040</u>	2.782	1.106	7.394	2.012	3.483	1.287	5.764	1.677
	36	1.470	0.743	2.679	1.080	<u>2.646</u>	1.088	2.689	<u>1.064</u>	7.551	2.031	3.103	1.148	4.755	1.467
	48	1.406	0.757	2.622	1.078	2.614	1.086	<u>2.324</u>	<u>0.999</u>	7.662	2.057	2.669	1.085	4.763	1.469
	60	1.827	0.862	2.857	1.157	2.804	1.146	2.802	<u>1.112</u>	7.931	2.100	<u>2.770</u>	1.125	5.264	1.564
	Avg.	1.595	0.790	2.846	1.144	<u>2.616</u>	1.090	2.649	<u>1.070</u>	7.635	2.050	3.006	1.161	5.136	1.544

by matrix decomposition as Equation (7)

$$\begin{aligned}\tilde{\mathcal{X}}_h^c &= \mathcal{X}_h + \mathcal{X}_h^T, \\ \tilde{\mathcal{X}}_h^c &= \mathcal{X}_h^c + N \approx UV + N,\end{aligned}\quad (7)$$

where $N \in \mathbb{R}^{n \times c}$ represents the noise and $\mathcal{X}_h^c \in \mathbb{R}^{n \times c}$ refers to the channel dependency after denoising. $U \in \mathbb{R}^{n \times m}$ and $V \in \mathbb{R}^{m \times c}$ ($m < c$) denote factorized channel interaction. We can use traditional methods such as truncated SVD (Rust, 1998) and NMF (Geng et al., 2021) to obtain \mathcal{X}_h^c . Here we provide a simple but effective factorizing method as

$$\mathcal{X}_h^c = \sigma(\tilde{\mathcal{X}}_h^c \cdot W_1^\top + b_1) \cdot W_2^\top + b_2, \quad (8)$$

where $W_1 \in \mathbb{R}^{m \times c}$, $W_2 \in \mathbb{R}^{c \times m}$ and σ is an activation function. Different from MLP-like architectures in the vision domain, here we emphasize the temporal and channel

redundancy of time series data and thus propose our factorization strategies. Notably, all the variants of our proposed MTS-Mixers can be mixed in an additive fashion if necessary. In practice, we only adopt the MLP-based MTS-Mixers via factorized temporal and channel mixing for the comparison with other baselines on forecasting tasks. See Appendix C.1 for more implementation details.

5. Experiments

5.1. Experimental setup

Datasets. We conduct extensive experiments on several public real-world benchmarks, covering economics, energy, traffic, weather, and infectious disease forecasting scenarios. Here is a detailed description of the datasets. (1) ECL¹

¹<https://archive.ics.uci.edu/ml/datasets/>

Table 2. The forecasting performance of different types of models on ECL dataset. The length of historical horizon is set as 96, and the MSE and MAE results are averaged from 4 different prediction lengths {96, 192, 336, 720}.

Backbone	Interaction capture	Low-rank property usage	MSE	MAE
MTS-Mixers	None	×	0.215	0.304
	+ Temporal MLP	×	0.189	0.280
	+ Channel MLP	×	0.185	0.285
	† Factorized MLP	✓	0.172	0.269
	Attention	×	0.215	0.316
	† Factorized Attention	✓	0.206	0.309
	+ Channel Factorization	✓	0.198	0.302
	Random Matrix	×	0.201	0.287
	Identity Matrix	×	0.201	0.286
	† Factorized Matrix	✓	0.195	0.286
+ Channel Factorization	✓	0.192	0.283	
FEDformer	Autocorrelation + DWT	✓	0.214	0.327
	+ Channel Factorization	✓	0.205	0.319
SCINet	Tree-Conv	✓	0.210	0.318
	+ Channel Factorization	✓	0.197	0.295

records the hourly electricity consumption of 321 customers from 2012 to 2014. (2) ETT (Electricity Transformer Temperature) (Zhou et al., 2021) consists of the data collected from electricity transformers, recording six power load features and oil temperature. (3) Traffic² contains the change of hourly road occupancy rates measured by hundreds of sensors on San Francisco Bay area freeways, which is collected from the California Department of Transportation. (4) PeMS04 (Chen et al., 2001) records the change of traffic flow at 307 sensors in the Bay Area over 2 months from Jan 1st, 2018 to Feb 28th, 2018. (5) Weather³ contains 21 meteorological indicators like humidity and pressure in the 2020 year from nearly 1600 locations in the U.S. (6) Exchange (Lai et al., 2018) is a collection of exchange rates among eight different countries from 1990 to 2016. (7) ILI⁴ records the weekly influenza-like illness (ILI) patients data from Centers for Disease Control and Prevention of the United States between 2002 and 2021, describing the ratio of patients observed with ILI and the total number of patients. For a fair comparison, we follow the same standard protocol and split all forecasting datasets into training, validation, and test sets by the ratio of 6:2:2 for the ETT dataset and 7:1:2 for the other datasets.

Baselines. We select six baseline methods for comparison, including four latest state-of-the-art Transformer-based models: Informer (Zhou et al., 2021), Autoformer (Wu et al., 2021), Pyraformer (Liu et al., 2022b), FEDformer (Zhou et al., 2022) and two latest non-Transformer models SCINet (Liu et al., 2022a) and DLinear (Zeng et al., 2022).

²<http://pems.dot.ca.gov/>

³<https://www.ncei.noaa.gov/data/local-climatological-data/>

⁴<https://gis.cdc.gov/grasp/fluview/fluportaldashboard.html>

All the baselines follow the same evaluation protocol for a fair comparison. See Appendix C.2 for more details.

Implementation details. Our method is trained with the L2 loss, using the Adam optimizer (Kingma & Ba, 2015). The training process is early stopped within 10 epochs. MSE $\frac{1}{n} \sum_{i=1}^n (\mathbf{y} - \hat{\mathbf{y}})^2$ and MAE $\frac{1}{n} \sum_{i=1}^n |\mathbf{y} - \hat{\mathbf{y}}|$ are adopted as evaluation metrics on all the benchmarks. All the models are implemented in PyTorch (Paszke et al., 2019) and trained/tested on a single Nvidia A100 40GB GPU for three times. See Appendix C for more experimental details and hyper-parameters setting.

5.2. Main results

To fairly compare the forecasting performance, we follow the same evaluation protocol, where the length of the historical horizon is set as 36 for ILI and 96 for the others. The prediction lengths are {24,36,48,60} for ILI and {96, 192, 336, 720} for others. Table 1 summarizes the results of multivariate time series forecasting on six datasets. The best results are highlighted in bold and the second best is underlined. MTS-Mixers achieves consistent state-of-the-art performance in all benchmarks. Especially compared with previous state-of-the-art results, MTS-Mixers yields a **18.1%** averaged MSE reduction in ECL, **10.8%** in Traffic, **17.0%** in PeMS04, comparable results in Exchange, **7.2%** in Weather and **39.0%** in ILI. The full benchmarks on the ETT are provided in Appendix A. See Appendix B for more results of univariate time series forecasting. Note that the strong baseline FEDformer generally performs well on large datasets while DLinear performs well on small datasets. MTS-Mixers outperforms in all benchmarks and prediction length settings, implying its strength in various

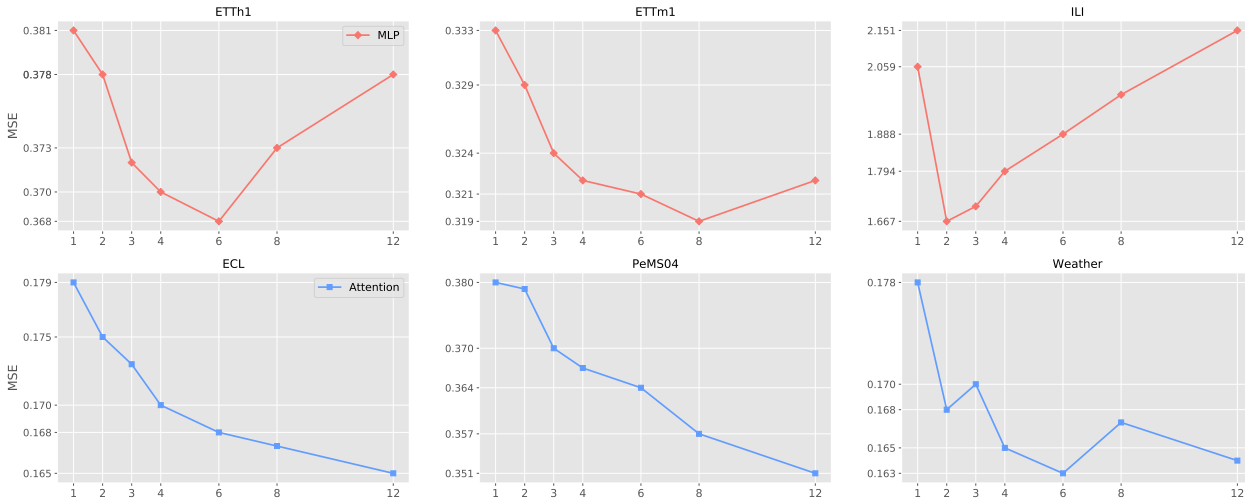


Figure 5. The impact of the hyper-parameter $s \in \{1, 2, 3, 4, 6, 8, 12\}$ which corresponds to the number of interleaved subsequences after downsampling the original time series data under the 96-96 setting. A lower MSE means better performance.

real-world scenarios.

5.3. Ablation studies

In this section, the ablation experiments are conducted, aiming at investigating: (1) the forecasting performance of the variants of MTS-Mixers; (2) the impact of factorized modules applied on other types of models, and (3) the detailed settings of temporal and channel factorization.

Variants of MTS-Mixers. Table 2 summarizes the forecasting performance of the variants of MTS-Mixers and other types of models on the ECL dataset over four different prediction lengths. Notice that the "None" interaction capture refers to a simple linear layer, which has been also mentioned in (Zeng et al., 2022). In general, our proposed MTS-Mixers based on MLP, attention, and random matrix all achieve better results than previous works, which verifies the effectiveness of this general framework on multivariate time series forecasting. All the variants of MTS-Mixers can gain consistent promotion via temporal and channel factorization, verifying that our proposed factorized strategies can be generalized to other models for capturing better temporal and channel interactions. Specifically, MTS-Mixers based on factorized MLP achieves the best prediction results, while the factorized attention outperforms the previous state-of-the-art Transformer-based models. MTS-Mixers based on factorized MLP does not need any positional or date-specific embedding, which guarantees the capture of temporal characteristics with less distortion. MTS-Mixers based on factorized attention outperforms vanilla attention with fewer parameters because the points in the subsequences after downsampling have more semantic information than before, which alleviates the over-fitting problem. Surprisingly,

MTS-Mixers based on random matrix achieves better results than attention, which further explains the non-necessity of attention mechanism in the capture of the temporal dependency. Note that the "identity" means the parameters of the random matrix are initialized to the identity matrix, which indicates the initialization of the random matrix has slight effects on the forecasting performance.

Notably, some methods like FEDformer and SCINet also have tried to utilize the low-rand property of time series data. Specifically, FEDformer determines required features in the frequency domain through random selection to obtain sparser temporal information. SCINet also applies downsampling to the original time series, recursively generating odd and even subsequences in a tree structure to learn multi-scale temporal dependencies. We apply the channel factorization to them and also achieve a consistent promotion.

Temporal factorization. Figure 5 demonstrates the impact of the hyper-parameter $s \in \{1, 2, 3, 4, 6, 8, 12\}$ which corresponds to the number of interleaved subsequences after downsampling the original time series data. Both MTS-Mixers based on MLP and attention achieve better forecasting performance after using temporal factorization. Notably, different datasets generally have different optimal s because they are collected from various scenarios and sensors with particular sampling rates. MTS-Mixers based on attention can obtain more promotions with larger s because it yields more semantic points with less redundancy.

To further improve the efficiency of temporal factorization, we can use only one temporal feature extractor (i.e. shared parameters) for different downsampled subsequences. As Table 4 shows, parameter-sharing temporal factorization can

Table 3. Running time (seconds) analysis for Transformer-based methods at different phases on the ECL dataset.

Phase	H	MTS-Mixers (MLP)	MTS-Mixers (attention)	FEDformer	Autoformer	Informer	Transformer
Training	96	10.3 ± 0.4	12.1 ± 0.7	72.4 ± 4.8	29.1 ± 0.7	24.4 ± 0.7	20.6 ± 0.9
	192	12.0 ± 0.4	14.5 ± 0.3	81.0 ± 3.6	31.4 ± 0.4	28.5 ± 1.1	22.8 ± 0.5
	336	14.8 ± 0.3	17.2 ± 0.1	100.2 ± 3.1	38.9 ± 0.5	33.2 ± 0.2	27.5 ± 0.8
	720	21.2 ± 0.6	23.0 ± 0.4	139.9 ± 1.0	65.0 ± 0.8	44.0 ± 1.1	39.0 ± 0.1
Inference	96	10.3 ± 0.5	9.4 ± 1.3	13.8 ± 0.3	12.5 ± 0.2	10.7 ± 1.3	10.5 ± 1.2
	192	12.8 ± 0.7	11.7 ± 0.4	18.6 ± 0.6	17.9 ± 1.3	16.1 ± 1.3	15.1 ± 1.1
	336	16.6 ± 0.9	17.0 ± 0.8	26.0 ± 0.7	27.5 ± 0.3	21.3 ± 1.5	21.0 ± 1.7
	720	26.2 ± 0.5	26.7 ± 0.6	44.9 ± 2.2	48.3 ± 2.2	40.1 ± 3.6	36.6 ± 0.2

significantly reduce the parameter quantity with a trade-off.

Table 4. The forecasting results of MTS-Mixers with shared parameters or not on the ETTm1 96-96 setting.

Backbone	s	MSE	MAE	params.
MLP	1	0.333	0.370	0.27M
MLP	8	0.319	0.357	0.28M
MLP (shared)	8	0.360	0.391	0.10M
Attention	1	0.358	0.389	4.23M
Attention	8	0.347	0.382	33.77M
Attention (shared)	8	0.348	0.383	4.23M

Table 5. The forecasting results of MTS-Mixers with different channel factorization strategies on the ECL 96-96 setting.

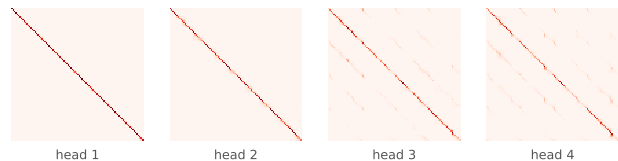
Decomposition	MSE	MAE
None	0.179	0.275
Truncated SVD (Rust, 1998)	0.162	0.254
NMF (Geng et al., 2021)	0.159	0.251
Channel Drop (Kong et al., 2021)	0.164	0.256
Factorized MLP (ours)	0.146	0.246

Channel factorization. As mentioned in Section 4, here we study the effects of other decomposition methods on channel factorization. Table 5 provides four denoising strategies, which all successfully alleviate the redundancy across channels and achieve higher prediction accuracy. Specifically, we only retain 10% of the maximum singular value in truncated SVD and follow the same setting of NMF in Geng et al. (2021). As for channel drop, we randomly discard 10% channels and set them as 0. The experiments prove the necessity of channel factorization in time series forecasting.

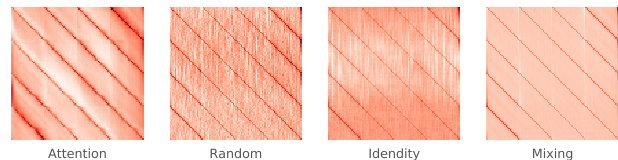
5.4. Model analysis

Prediction patterns analysis. As Figure 6 shows, we investigate what patterns the models learn in forecasting tasks. Specifically, most of the heads in attention of vanilla Transformer may hardly capture any useful information. Instead,

the variants of MTS-Mixers consistently learn the similar mapping matrix with periodic characteristics. We provide additional analysis and visualisation of weights for other datasets in Appendices D and E.



(a) Visual analysis of Transformer attention on ECL.



(b) Visual analysis of MTS-Mixers on ECL.

Figure 6. The visual analysis of Transformer and MTS-Mixers on the ECL. Only one layer of the encoder is used for each model.

Runtime analysis. We conduct runtime analysis for Transformer based methods on the ECL dataset. Each of them is run three times for one epoch. As Table 3 shows, our proposed MTS-Mixers achieve better efficiency in the training and inference stages. Although some previous works have emphasized their contribution to reducing the complexity of attention, their operational efficiency is not high due to a bulk of additional processing such as Wavelet Transform, reminding us to challenge their claimed efficiency.

6. Conclusion

This paper proposes MTS-Mixers, a general framework for multivariate time series forecasting. We conducted an extensive study to investigate the real contribution and deficiencies of attention mechanisms on the performance of time series forecasting. The experimental results have demonstrated that attention is unnecessary for capturing temporal

dependencies, and the redundancy in time series data affects the forecasting performance. Furthermore, our proposed temporal and channel factorization strategies leverage the low-rank property of time series data and have achieved state-of-the-art results on several real-world datasets with higher efficiency. Model analysis on patterns that the models have learned indicates that the mapping between the input and output sequences may be the key we need.

References

- Angryk, R. A., Martens, P. C., Aydin, B., Kempton, D. J., Mahajan, S. S., Basodi, S., Ahmadzadeh, A., Cai, X., Boubrahimi, S. F., Hamdi, S. M., Schuh, M. A., and Georgoulis, M. K. Multivariate time series dataset for space weather data analytics. *Scientific Data*, 7, 2020.
- Ariyo, A. A., Adewumi, A. O., and Ayo, C. K. Stock price prediction using the arima model. *2014 UKSim-AMSS 16th International Conference on Computer Modelling and Simulation*, pp. 106–112, 2014.
- Bai, S., Kolter, J. Z., and Koltun, V. An empirical evaluation of generic convolutional and recurrent networks for sequence modeling. *ArXiv*, abs/1803.01271, 2018.
- Challu, C., Olivares, K. G., Oreshkin, B. N., Garza, F., Mergenthaler-Canseco, M., and Dubrawski, A. W. N-hits: Neural hierarchical interpolation for time series forecasting. *ArXiv*, abs/2201.12886, 2022.
- Chen, C., Petty, K. F., Skabardonis, A., Varaiya, P. P., and Jia, Z. Freeway performance measurement system: Mining loop detector data. *Transportation Research Record*, 1748:102 – 96, 2001.
- Child, R., Gray, S., Radford, A., and Sutskever, I. Generating long sequences with sparse transformers. *ArXiv*, abs/1904.10509, 2019.
- Diao, Q., Jiang, Y., Wen, B., Sun, J., and Yuan, Z. Metaformer: A unified meta framework for fine-grained recognition. *ArXiv*, abs/2203.02751, 2022.
- Geng, Z., Guo, M.-H., Chen, H., Li, X., Wei, K., and Lin, Z. Is attention better than matrix decomposition? *ArXiv*, abs/2109.04553, 2021.
- Hendrycks, D. and Gimpel, K. Gaussian error linear units (gelus). *arXiv: Learning*, 2016.
- Khan, Z. A., Hussain, T., Ullah, A., Rho, S., Lee, M. Y., and Baik, S. W. Towards efficient electricity forecasting in residential and commercial buildings: A novel hybrid cnn with a lstm-ae based framework. *Sensors (Basel, Switzerland)*, 20, 2020.
- Kim, T., Kim, J., Tae, Y., Park, C., Choi, J., and Choo, J. Reversible instance normalization for accurate time-series forecasting against distribution shift. In *International Conference on Learning Representations*, 2022.
- Kingma, D. P. and Ba, J. Adam: A method for stochastic optimization. *CoRR*, abs/1412.6980, 2015.
- Kong, X., Liu, X., Gu, J., Qiao, Y., and Dong, C. Re-flash dropout in image super-resolution. *2022 IEEE/CVF Conference on Computer Vision and Pattern Recognition (CVPR)*, pp. 5992–6002, 2021.
- Lai, G., Chang, W.-C., Yang, Y., and Liu, H. Modeling long- and short-term temporal patterns with deep neural networks. *The 41st International ACM SIGIR Conference on Research & Development in Information Retrieval*, 2018.
- Lee-Thorp, J., Ainslie, J., Eckstein, I., and Ontañón, S. Fnet: Mixing tokens with fourier transforms. In *North American Chapter of the Association for Computational Linguistics*, 2021.
- Li, S., Jin, X., Xuan, Y., Zhou, X., Chen, W., Wang, Y.-X., and Yan, X. Enhancing the locality and breaking the memory bottleneck of transformer on time series forecasting. *ArXiv*, abs/1907.00235, 2019.
- Liu, M., Zeng, A., Chen, M., Xu, Z., LAI, Q., Ma, L., and Xu, Q. SCINet: Time series modeling and forecasting with sample convolution and interaction. In Oh, A. H., Agarwal, A., Belgrave, D., and Cho, K. (eds.), *Advances in Neural Information Processing Systems*, 2022a. URL <https://openreview.net/forum?id=AyajSjTazmg>.
- Liu, S., Yu, H., Liao, C., Li, J., Lin, W., Liu, A. X., and Dastdar, S. Pyraformer: Low-complexity pyramidal attention for long-range time series modeling and forecasting. In *International Conference on Learning Representations*, 2022b.
- Ma, J., Shou, Z., Zareian, A., Mansour, H., Vetro, A., and Chang, S.-F. Cdsa: Cross-dimensional self-attention for multivariate, geo-tagged time series imputation. *ArXiv*, abs/1905.09904, 2019.
- Oreshkin, B. N., Carpov, D., Chapados, N., and Bengio, Y. N-beats: Neural basis expansion analysis for interpretable time series forecasting. *ArXiv*, abs/1905.10437, 2019.
- Paszke, A., Gross, S., Massa, F., Lerer, A., Bradbury, J., Chanan, G., Killeen, T., Lin, Z., Gimelshein, N., Antiga, L., Desmaison, A., Köpf, A., Yang, E., DeVito, Z., Raison, M., Tejani, A., Chilamkurthy, S., Steiner, B., Fang, L., Bai, J., and Chintala, S. Pytorch: An imperative style, high-performance deep learning library. In *NeurIPS*, 2019.

- Rust, B. W. Truncating the singular value decomposition for ill-posed problems. 1998.
- Song, H.-Z., Rajan, D., Thiagarajan, J. J., and Spanias, A. Attend and diagnose: Clinical time series analysis using attention models. In *AAAI*, 2018.
- Tay, Y., Bahri, D., Metzler, D., Juan, D.-C., Zhao, Z., and Zheng, C. Synthesizer: Rethinking self-attention in transformer models. In *International Conference on Machine Learning*, 2020.
- Tolstikhin, I. O., Houlsby, N., Kolesnikov, A., Beyer, L., Zhai, X., Unterthiner, T., Yung, J., Keysers, D., Uszkoreit, J., Lucic, M., and Dosovitskiy, A. Mlp-mixer: An all-mlp architecture for vision. In *Neural Information Processing Systems*, 2021.
- Vaswani, A., Shazeer, N. M., Parmar, N., Uszkoreit, J., Jones, L., Gomez, A. N., Kaiser, L., and Polosukhin, I. Attention is all you need. *ArXiv*, abs/1706.03762, 2017.
- Woo, G., Liu, C., Sahoo, D., Kumar, A., and Hoi, S. C. H. Etsformer: Exponential smoothing transformers for time-series forecasting. *ArXiv*, abs/2202.01381, 2022.
- Wu, H., Xu, J., Wang, J., and Long, M. Autoformer: Decomposition transformers with auto-correlation for long-term series forecasting. In *Neural Information Processing Systems*, 2021.
- Zeng, A., Chen, M.-H., Zhang, L., and Xu, Q. Are transformers effective for time series forecasting? *ArXiv*, abs/2205.13504, 2022.
- Zhang, G. P. Time series forecasting using a hybrid arima and neural network model. *Neurocomputing*, 50:159–175, 2003.
- Zhou, H., Zhang, S., Peng, J., Zhang, S., Li, J., Xiong, H., and Zhang, W. Informer: Beyond efficient transformer for long sequence time-series forecasting. *ArXiv*, abs/2012.07436, 2021.
- Zhou, T., Ma, Z., Wen, Q., Wang, X., Sun, L., and Jin, R. Fedformer: Frequency enhanced decomposed transformer for long-term series forecasting. *ArXiv*, abs/2201.12740, 2022.

A. Full Benchmark on the ETT Datasets

Table 6. The full multivariate time series forecasting benchmarks of ETT datasets. The length of historical horizon is set as 96 and the prediction lengths are {96, 192, 336, 720} for all the datasets. The best results are highlighted in **bold**. The second best is underlined.

Method	MTS-Mixers		FEDformer		DLinear		SCINet		Pyraformer		Autoformer		Informer		
Metric	MSE	MAE	MSE	MAE	MSE	MAE	MSE	MAE	MSE	MAE	MSE	MAE	MSE	MAE	
ETTh1	96	0.368	0.393	<u>0.376</u>	0.419	0.386	<u>0.400</u>	0.404	0.415	0.664	0.612	0.449	0.459	0.865	0.713
	192	0.419	0.425	<u>0.420</u>	0.448	0.437	<u>0.432</u>	0.456	0.445	0.790	0.681	0.500	0.482	1.008	0.792
	336	<u>0.466</u>	0.453	0.459	0.465	0.481	<u>0.459</u>	0.519	0.481	0.891	0.738	0.521	0.496	1.107	0.809
	720	0.473	0.470	<u>0.506</u>	<u>0.507</u>	0.519	0.516	0.564	0.528	0.963	0.782	0.514	0.512	1.181	0.865
	Avg.	0.432	0.435	<u>0.440</u>	0.460	0.456	<u>0.452</u>	0.486	0.467	0.827	0.703	0.496	0.487	1.040	0.795
ETTh2	96	0.319	0.357	0.379	0.419	<u>0.345</u>	<u>0.372</u>	0.350	0.385	0.543	0.510	0.505	0.475	0.672	0.571
	192	0.363	0.384	0.426	0.441	<u>0.380</u>	<u>0.389</u>	0.382	0.400	0.557	0.537	0.553	0.496	0.795	0.669
	336	0.397	0.408	0.445	0.459	<u>0.413</u>	<u>0.413</u>	0.419	0.425	0.754	0.655	0.621	0.537	1.212	0.871
	720	0.456	0.445	0.543	0.490	<u>0.474</u>	<u>0.453</u>	0.494	0.463	0.908	0.724	0.671	0.561	1.166	0.823
	Avg.	0.384	0.399	0.448	0.452	<u>0.403</u>	<u>0.407</u>	0.411	0.418	0.691	0.607	0.588	0.517	0.961	0.734
ETTh1	96	0.303	0.352	0.358	0.397	0.333	0.387	<u>0.312</u>	<u>0.355</u>	0.645	0.597	0.346	0.388	3.755	1.525
	192	0.390	0.407	0.429	0.439	0.477	0.476	<u>0.401</u>	<u>0.412</u>	0.788	0.683	0.456	0.452	5.602	1.931
	336	<u>0.436</u>	<u>0.437</u>	0.496	0.487	0.594	0.541	0.413	0.432	0.907	0.747	0.482	0.486	4.721	1.835
	720	0.426	0.440	<u>0.463</u>	<u>0.474</u>	0.831	0.657	0.490	0.483	0.963	0.783	0.515	0.511	3.647	1.625
	Avg.	0.389	0.409	0.437	0.449	0.559	0.515	<u>0.404</u>	<u>0.421</u>	0.826	0.703	0.450	0.459	4.431	1.729
ETTh2	96	0.177	0.261	0.203	0.287	<u>0.193</u>	0.292	0.201	<u>0.280</u>	0.435	0.507	0.255	0.339	0.365	0.453
	192	0.240	0.300	<u>0.269</u>	<u>0.328</u>	0.284	0.362	0.283	<u>0.331</u>	0.730	0.673	0.281	0.340	0.533	0.563
	336	0.304	0.343	<u>0.325</u>	<u>0.366</u>	0.369	0.427	<u>0.318</u>	<u>0.352</u>	1.201	0.845	0.339	0.372	1.363	0.887
	720	0.395	0.397	<u>0.421</u>	<u>0.415</u>	0.554	0.522	0.439	0.423	3.625	1.451	0.422	0.419	3.379	1.388
	Avg.	0.279	0.325	<u>0.304</u>	0.349	0.350	0.401	0.310	<u>0.347</u>	1.498	0.869	0.324	0.368	1.410	0.823

Table 6 shows the full multivariate time series forecasting benchmarks of four ETT datasets, including the hourly recorded ETTh1 and ETTh2; minutely recorded ETTm1 and ETTm2. MTS-Mixers also achieve consistent state-of-the-art performance in four ETT benchmarks. Specifically, MTS-Mixers yields a **1.8%** averaged MSE reduction in ETTh1, **4.7%** in ETTm1, **3.7%** in ETTh2 and **8.2%** in ETTm2 compared with the second best results.

B. Univariate Time Series Forecasting

Table 7. The univariate time series forecasting results. The length of historical horizon is set as 96 and the prediction lengths are {96, 192, 336, 720} for all the datasets. The best results are highlighted in **bold**. The second best is underlined.

Method	MTS-Mixers		DLinear		FEDformer		SCINet		N-HiTs		N-BEATS		Autoformer		
Metric	MSE	MAE	MSE	MAE	MSE	MAE	MSE	MAE	MSE	MAE	MSE	MAE	MSE	MAE	
Exchange	96	0.096	0.226	0.110	0.264	0.140	0.295	<u>0.101</u>	<u>0.238</u>	0.114	0.248	0.156	0.299	0.153	0.306
	192	0.199	0.335	<u>0.223</u>	0.383	0.278	0.411	<u>0.223</u>	<u>0.351</u>	0.250	0.387	0.669	0.665	0.302	0.424
	336	0.389	0.471	<u>0.405</u>	0.509	0.515	0.554	<u>0.429</u>	<u>0.493</u>	0.434	0.516	0.611	0.605	0.609	0.615
	720	1.074	0.791	1.044	<u>0.782</u>	1.319	0.891	1.094	0.796	<u>1.061</u>	0.773	1.111	0.860	1.261	0.873
	Avg.	0.440	0.456	<u>0.446</u>	0.485	0.563	0.538	0.462	<u>0.470</u>	0.465	0.481	0.637	0.607	0.581	0.555
ETTh2	96	0.065	0.184	0.071	<u>0.194</u>	<u>0.069</u>	0.198	0.074	0.197	0.092	0.232	0.082	0.219	0.099	0.241
	192	0.100	0.235	0.104	0.238	<u>0.103</u>	0.246	<u>0.103</u>	<u>0.237</u>	0.128	0.276	0.120	0.268	0.132	0.276
	336	0.131	0.276	0.143	0.288	<u>0.131</u>	<u>0.281</u>	0.135	0.280	0.165	0.314	0.226	0.370	0.154	0.305
	720	0.184	0.334	0.192	0.336	<u>0.185</u>	<u>0.331</u>	<u>0.185</u>	0.335	0.243	0.397	0.188	0.338	0.205	0.353
	Avg.	0.120	0.257	0.128	0.264	<u>0.122</u>	0.264	0.124	<u>0.262</u>	0.157	0.305	0.154	0.299	0.148	0.294

Table 7 provides the univariate time series forecasting results on two typical datasets. Here we include two baselines

N-HiTs (Challu et al., 2022) and N-BEATS (Oreshkin et al., 2019) which are widely used in univariate benchmarks. Notably, for univariate time series forecasting, we remove the channel factorization module in MTS-Mixers. MTS-Mixers yields a **1.3%** averaged MSE reduction in Exchange and **1.6%** in ETTm2 univariate benchmarks, proving the effectiveness of our proposed temporal factorization strategy.

C. Experimental Details

C.1. Reproduction Details for MTS-Mixers

As shown in Figure 2, we have proposed three specific implementations of MTS-Mixers. For attention-based MTS-Mixer, we do not use convolution operation to obtain tokens but directly capture temporal dependency on each channel via multi-head self-attention. The number of the head is set as the least prime factor of c which is the number of channels of the time series instance $\mathcal{X} \in \mathbb{R}^{n \times c}$. The feedforward neural network (FFN) consists of two fully-connected layers and a GELU (Hendrycks & Gimpel, 2016) activation. The number of hidden states in FFN is selected from $\{64, 512, 2048\}$ which corresponds to c of different datasets. For matrix-based MTS-Mixer, we provide two initialization forms, including random and identity matrix initialization. For MLP-based MTS-Mixer, the temporal and channel MLPs both contain two linear layers with a GELU activation. The number of hidden states is set as 512 for temporal MLP and m for channel MLP. The number of stacked units in MTS-Mixers for capturing temporal and channel interaction is all set as 2 for a fair comparison. We adopt reversible instance normalization (Kim et al., 2022) rather than disentanglement to alleviate the distribution shift problem.

Temporal factorization. Figure 7 illustrates an example of temporal factorization where we down-sample the original time series into two interleaved subsequences. In practice, We apply equidistant down-sampling in the original time series $\mathcal{X} \in \mathbb{R}^{n \times c}$ as

$$\mathcal{X}_{h,i} = \tilde{\mathcal{X}}_h[i-1::s, :], \quad 1 \leq i \leq s, \quad (9)$$

where i denotes the i -th subsequence and $[\cdot]$ means a slice operation. We perform a grid search over the number of interleaved subsequences $s \in \{1, 2, 3, 4, 6, 8, 12\}$ on all benchmarks.

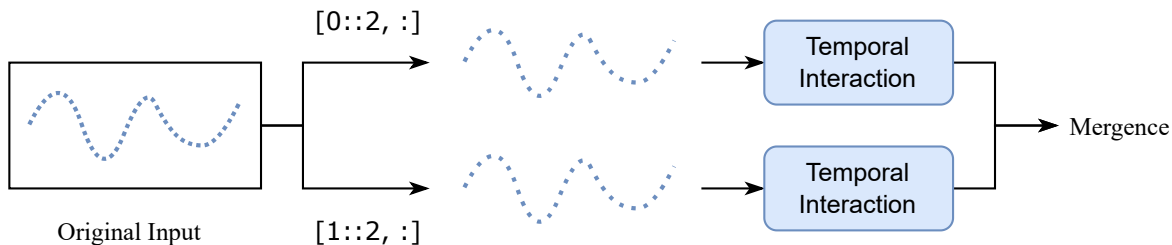


Figure 7. An example of temporal factorization when $s = 2$.

Channel factorization. As mentioned in Equation (7) and (8), we use a channel MLP to learn factorized channel interaction $\mathcal{X}_h^c = UV$ where $U \in \mathbb{R}^{n \times m}$ and $V \in \mathbb{R}^{m \times c}$ ($m < c$). We perform a grid search over $m \in \{0, 16, 64\}$ (0 means no interaction among channels).

C.2. Details on Benchmark Tasks and Baselines

We conduct experiments on ten time series datasets and all of them follow the same pre-processing protocol in (Zhou et al., 2021). The random seed is set as 1024 in the training phase. Table 8 provides the initial learning rate and batch size used in different datasets. For time series forecasting baselines, the results of FEDformer, DLinear, SCINet, Autoformer, and Informer are based on our reproduction. The hyper-parameters are the same as their suggestions in the original paper.

Table 8. The hyper-parameters used in different datasets.

Hyper-parameters	ECL	Traffic	PeMS04	Exchange	Weather	ILI	ETT
Learning rate	1e-3	5e-2	5e-3	5e-4	1e-3	1e-2	5e-3
Batch size	16	16	16	8	16	32	32

D. MTS-Mixers Weights Visualization on Different Datasets

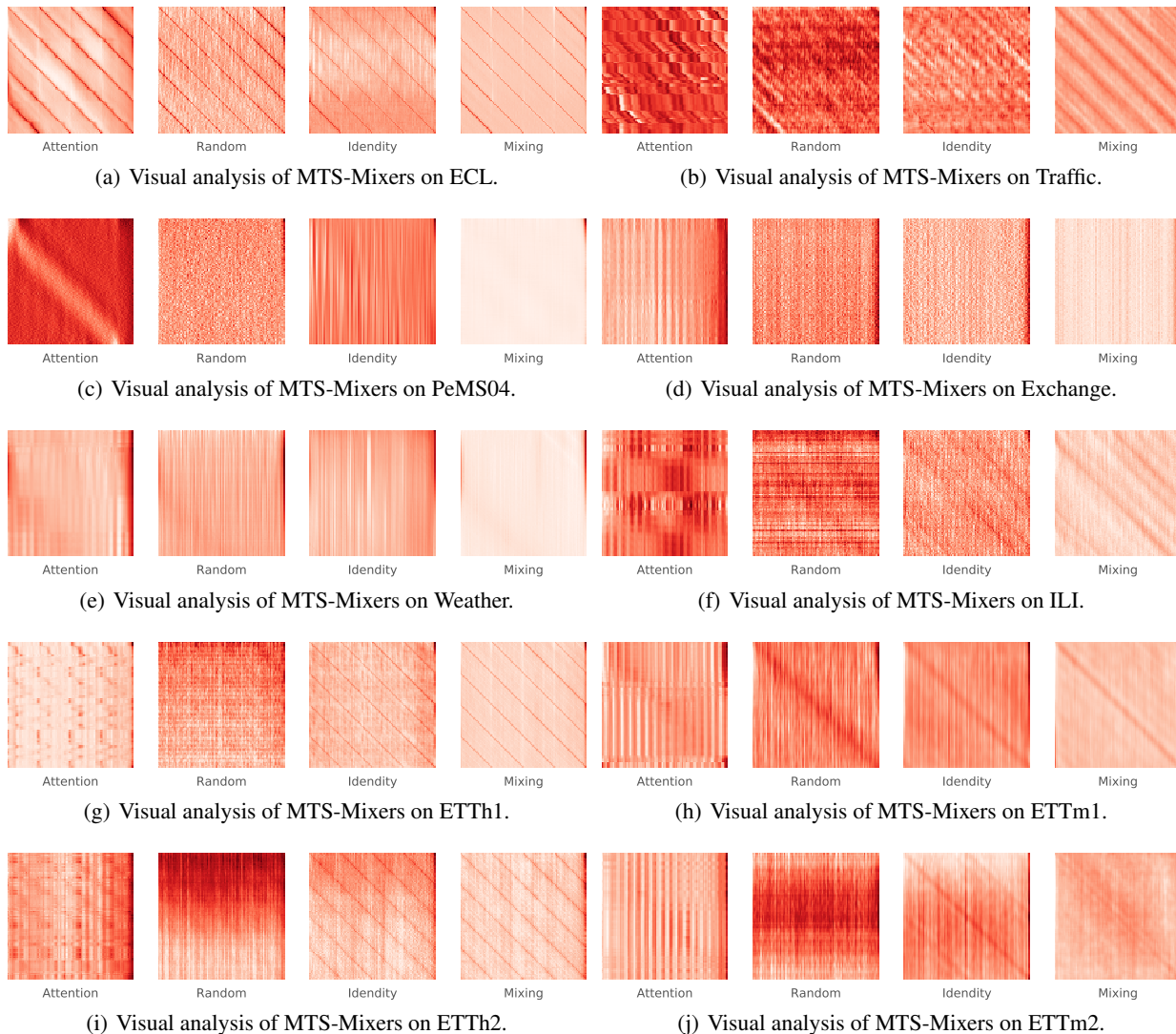


Figure 8. The visual analysis of MTS-Mixers on different datasets. Only one layer of the stacked block is used for better illustration.

E. From vanilla Transformer to Attention-based MTS-Mixers

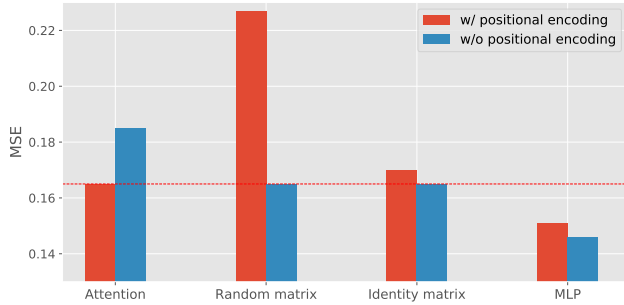
Compared with the vanilla Transformer, we remove its decoder and use one linear layer to model the map between learned features and the target sequence. Then we remove the tokenization generally used in Transformer-based frameworks and directly learn temporal information via the self-attention mechanism. Thus, the modeling of temporal and channel interaction is decoupled. Finally, we apply our proposed temporal factorization strategy to the attention, which is an attention-based MTS-Mixer. Table 9 provides the forecasting results from vanilla Transformer to attention-based MTS-Mixer on the ECL dataset, proving the effectiveness of these modifications.

F. The Impact of Positional Encoding

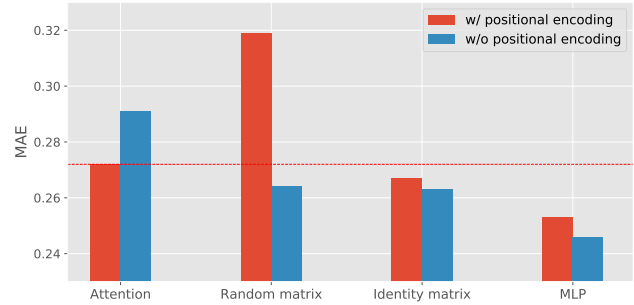
Although our proposed attention-based MTS-Mixer outperforms other Transformer-based methods, there is still a gap between attention and matrix-based or MLP-based MTS-Mixer. We argue that it is the distortion caused by positional encoding to capture temporal information. Figure 9 shows the results of different MTS-Mixers with or without positional encoding on the ECL dataset. Only attention-based MTS-Mixer require positional encoding, while matrix-based and MLP-based MTS-Mixers degrade performance if adding ordering information.

Table 9. From vanilla Transformer to Attention-based MTS-Mixers on the ECL dataset under the 96-96 setting.

Variants	MSE	MAE	Promotion
Vanilla Transformer	0.201	0.307	/
Remove the decoder	0.188	0.293	+6.5%
Temporal and channel decoupling	0.179	0.284	+10.9%
Factorized Attention	0.165	0.272	+17.9%



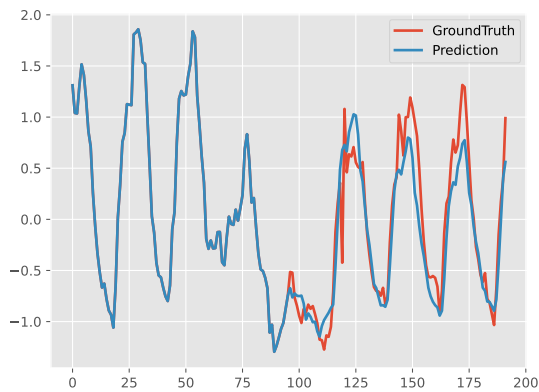
(a) MSE of MTS-Mixers w/ or w/o PE.



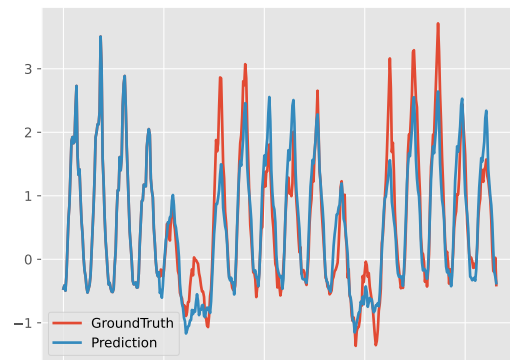
(b) MAE of of MTS-Mixers w/ or w/o PE.

Figure 9. The results of MTS-Mixers with or without positional encoding on the ECL dataset under the 96-96 setting. The form of positional encoding follows (Zhou et al., 2021). Lower MSE and MAE mean better forecasting performance.

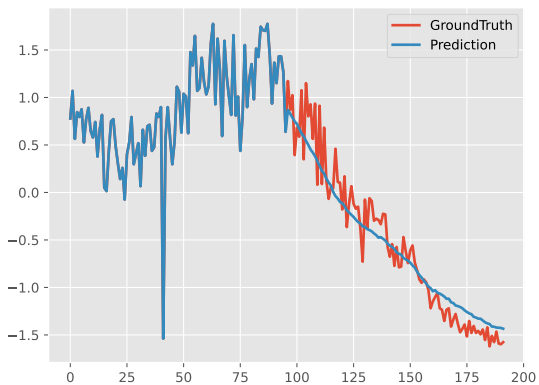
G. Forecasting Showcases



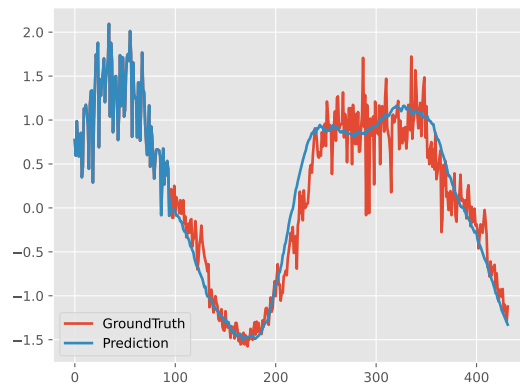
(a) Given 96 to predict 96 steps on the ECL.



(b) Given 96 to predict 336 steps on the ECL.



(c) Given 96 to predict 96 steps on the PeMS04.



(d) Given 96 to predict 336 steps on the PeMS04.